

Effects of Pre-Processing on Reverse Time Migration: a North Sea study

Ian F. Jones

First Break, **26**, no.6, 73-80

corresponding author

ian.jones@iongeo.com

ION GX Technology EAME
180 High Street, Egham
Surrey TW20 9DY, UK

The Effects of Pre-Processing on Reverse Time Migration: a North Sea study

Ian F. Jones

corresponding author: ian.jones@iongeo.com

Abstract

Almost all conventional pre-processing is conceived of with one-way wave propagation in-mind. If we take into account the existence of two-way wave propagation arrival events, then many of the underlying assumptions of moveout behaviour implicit in some pre-processing techniques must be re-evaluated.

Using 2D synthetic data, we demonstrate that the moveout behaviour of double bounce arrivals (a class of two-way propagating events) can be compromised by pre-processing designed to remove events exhibiting 'anomalous' moveout behaviour.

These observations are of interest to us, as we are now beginning to employ two-way migration schemes to image complex structures. However, if we continue to use conventional pre-processing techniques, we run the risk of removing the very events we are trying to image.

The observations made on the basis of synthetic modelled data, are extended in this work to real data examples, all from the North Sea, where in the central graben, we commonly have steep piercement salt diapir structures, which are good candidates for producing useful double bounce arrivals, which can be imaged using RTM.

Introduction

The speed and cost effectiveness of contemporary computer systems now permits us to implement more general algorithmic solutions of the wave equation (Whitmore, 1983, Baysal et al, 1983, McMechan, 1984, Bednar et al 2003, Yoon et al 2003, Shan & Biondi 2004, Zhou et al, 2006, Zhang et al, 2006). The restriction to one-way propagation can be lifted, and data migrated so as to take advantage of more esoteric propagation paths, such as turned rays, double bounce arrivals, and potentially multiples (Mittet, 2006)

However, in order to take advantage of these improved algorithms, we must ensure that the data input to migration have not been compromised in any way. Specifically, in this work we address the moveout behaviour of double bounce events (Hawkins et al, 1995, Bernitsas et al, 1997, Cavalca & Lailly, 2005), and note how many conventional pre-processing algorithms can damage these arrivals, thus rendering some aspects of any subsequent high-end migration superfluous.

We commence our analysis by reviewing some of the conclusions of preliminary work studying synthetic data (Jones, 2008), which discussed the moveout behaviour of turning waves (Hale, et al, 1992) and simple double bounce events (also referred to as 'prism waves' by some authors). For ease of demonstration, we firstly employ a ray-trace package, with which we can model individual selected arrivals, and later create more complex synthetic data using an elastic finite difference (FD) package. Some brief details of these packages are given.

After investigating the moveout behaviour of the simple models, we move-on to a model representing a complex North Sea salt dome structure (Davison, et al 2000, Thomson, 2004; Farmer, et al 2006). We show the effect of various conventional pre-processing steps on double bounce arrivals, and carry these analyses through to migration with an 2D RTM algorithm capable of imaging the double bounce arrivals.

We then extend this analysis and demonstration-of-principle from the 2D synthetic data to real data, where we see similar classes of event, and the same degradation of double bounce arrivals shown in the synthetic trials.

Work Program

1) Using a workstation-based 2D modelling system developed by Don Larson (GXII), we generated acoustic ray-traced CMP data as control to identify various individual arrivals. The initial data creation and analysis was performed for simple geometries, then repeated for a complex North Sea salt diapir model (2ms sampling, peak-frequency ~35Hz, shot interval 50m, CMP interval 6.25m, 6km maximum offset).

2) We then generated more 'realistic' elastic FD shot gather data for the complex North Sea salt diapir model. These modelled data included attenuation with an absorbing boundary condition, using same vertical interval velocity model as the ray-traced model for 1ms data (resampled to 4ms for processing), and a peak-frequency of ~17Hz. In this study we have used an absorbing surface boundary; hence the FD data have no free-surface multiples (whereas the ray-trace data does). The explicit 2D/3D elastic wave propagation code is 4th-order accurate in space and 2nd-order accurate in time, and is based on the elastodynamic formulation of the wave equation on a staggered grid (Madariaga, 1976; Virieux, 1986; Levander, 1988; Larsen & Grieger, 1998).

3) Pre-process the FD data using 'conventional' data processing flows that are likely to damage double bounce events, including:

- Tau-P mute for backscattered noise
- Radon demultiple
- CMP domain Apex Shifted Multiple Attenuation (ASMA)

4) 2D RTM after each pre-processing flow (all data input to the RTM's have a mute on the direct arrival), and assess the preservation of double bounce (prism wave) arrivals in the resultant images.

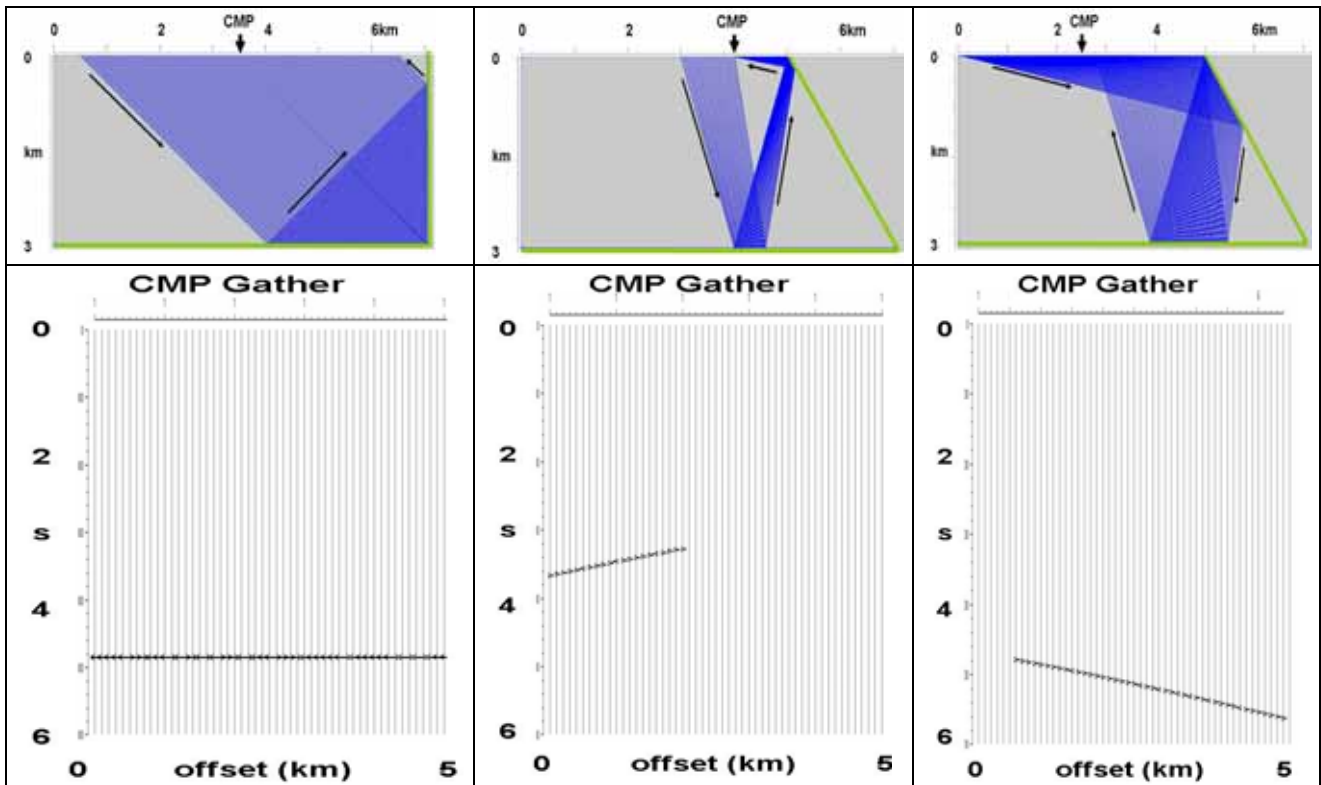
The Modelling

We commence by looking at three simple scenarios:

- a simple right-angle corner reflector
- an acute angle reflector (non-crossing rays)
- an acute angle reflector (crossing rays)

(for an obtuse angle geometry, we don't have double bounce arrivals for this layout: we would need extremely long offsets and large arrival times)

In figures 1 - 3, we show these three scenarios. It is clear that the moveout behaviour does not conform to what we expect for 'normal' one-way arrivals paths, but more closely resembles events such as those resulting from scattered energy or diffracted multiples. We know that for simple quasi-1D cylindrical models that all co-axially recorded events in a CMP gather will appear with their apex at zero offset. It is this observation that guides the design principle of various multiple suppression techniques and the justification to muting in Tau-P space to suppress backscattered energy.



Figures 1-3: In each example we show the model horizons in green, with sample ray paths, arrows indicating propagation direction. Below each frame we see the resulting CMP gather with the arrival events shown. Figure 1: Right angle corner reflector travel time is constant with offset: i.e. no moveout. Figure 2: Acute angle; non-crossing events. Arrivals are only present on the near offsets, with arrival time decreasing with offset. Figure 3: Acute angle; crossing events. Arrivals are present on most offsets, with arrival time increasing with offset

We now look at a full synthetic data set created along a 2D crestal line of the 3D production model representing our North Sea example, and show the effects of various pre-processing techniques on these data. For the geometry here, we have:

- a single bounce at the flat-lying part of a reflector
- a single bounce at the dipping part of this reflector
- a non-crossing double bounce involving the flat and dipping reflectors
- a crossing double bounce involving the flat and dipping reflectors (not shown in figure 4, so as to avoid clutter)
- ray paths passing into the salt, with an internal reflection at the steep salt wall, and a second bounce outside the salt from the flat or steep reflectors (not considered here, as they have relatively low amplitude due to the transmission coefficients at the salt wall).

These ray paths and an associated CMP gather are shown in figure 4. The velocity model shown is based on a 2D crestal line taken from an actual 3D North Sea example (Farmer, et al 2006). The production project in that case was anisotropic using VTI 3D RTM code, but for simplicity, here we are using 2D isotropic modeling and 2D isotropic RTM.

We can clearly see from the ray-tracing exercises, which are the single and which are the double bounce events illuminating the salt flank. We can also identify a class of events passing through the salt body itself and illuminating the salt flank, but these are weak due to the impedance contrast at the salt boundary, and will not be discussed here (and are also omitted from the diagram to avoid clutter). Figures 6 & 7 show the interval velocity model and associated elastic FD stack (the stack is produced using the RMS velocity associated with the interval velocity model, and not on stacking velocity analysis, and has a mute of the direct arrival energy).

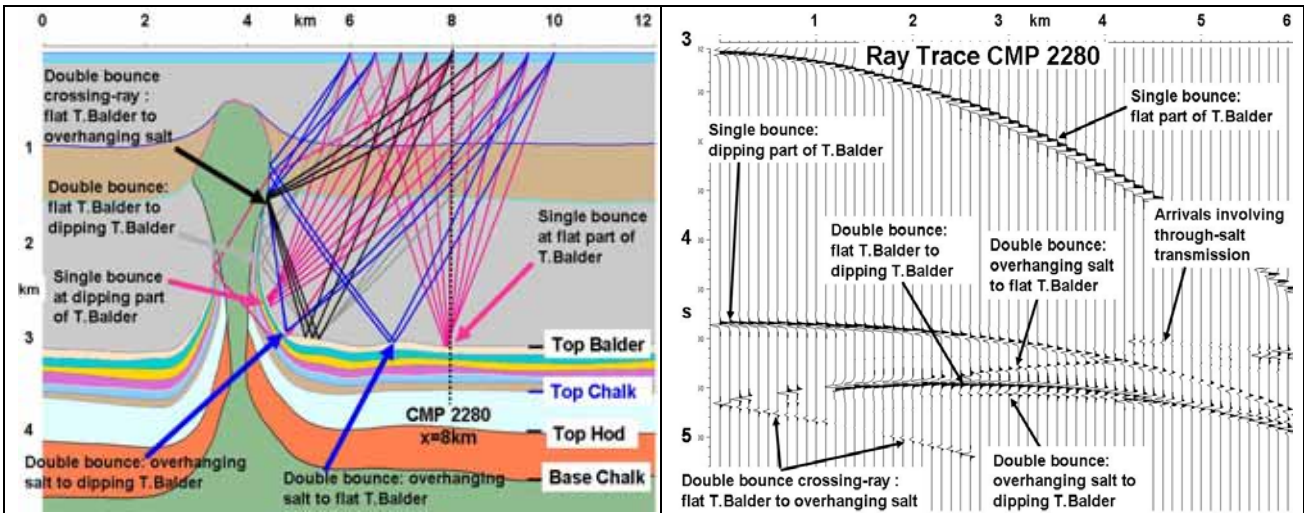


Figure 4, plot of a few sparse rays shown against the interval velocity model. The sediment velocity ranges from about 1900m/s to 2200m/s, with some shallow impedance contrast events. The absence of a strong sediment gradient precludes turning rays in the sediments, although a strong compaction velocity gradient below the Top Balder and top Chalk does produce turning rays. The salt velocity (green) is 4500m/s, and the chalk velocity is between 5500m/s and 6000m/s. A single CMP gather (from the surface location at 8km) is shown in figure 5.

Figure 7b shows an enlargement of the diffraction tails on the right flank of the dome indicated by the box in figure 7a. We see the ray-trace modelling with and without double bounce events, permitting us to identify where they occur in the section. Also shown is the full elastic FD result.

These differences can be seen more clearly in an individual CMP gather. Figures 8 & 9 show a gather at CMP location 2240, for ray-tracing including double bounces, and full elastic FD modelling. (It is clear here why it is necessary to perform ray trace modelling for individual sets of events, as otherwise it is too difficult to understand what we're seeing in the FD data).

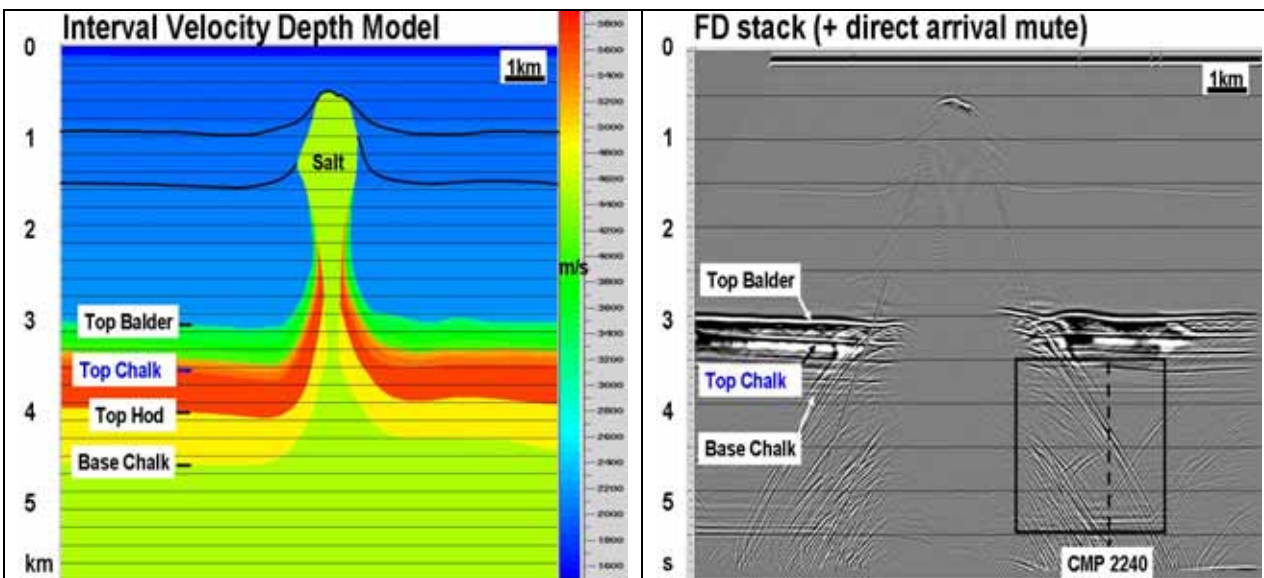


Figure 6: the velocity depth model, with main horizons indicated. Figure 7 shows the brute stack of the FD data. The direct arrivals have been muted. The indicated box near CMP 2240 is show in detail in the next figure.

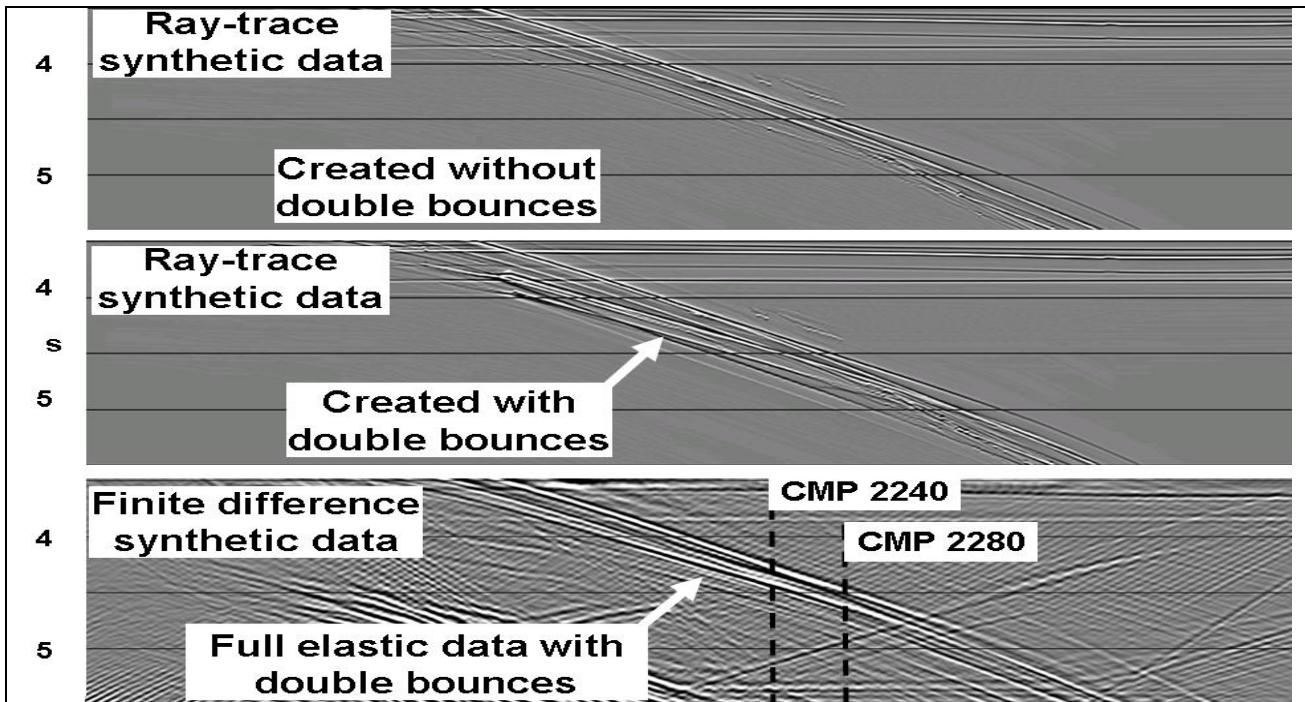
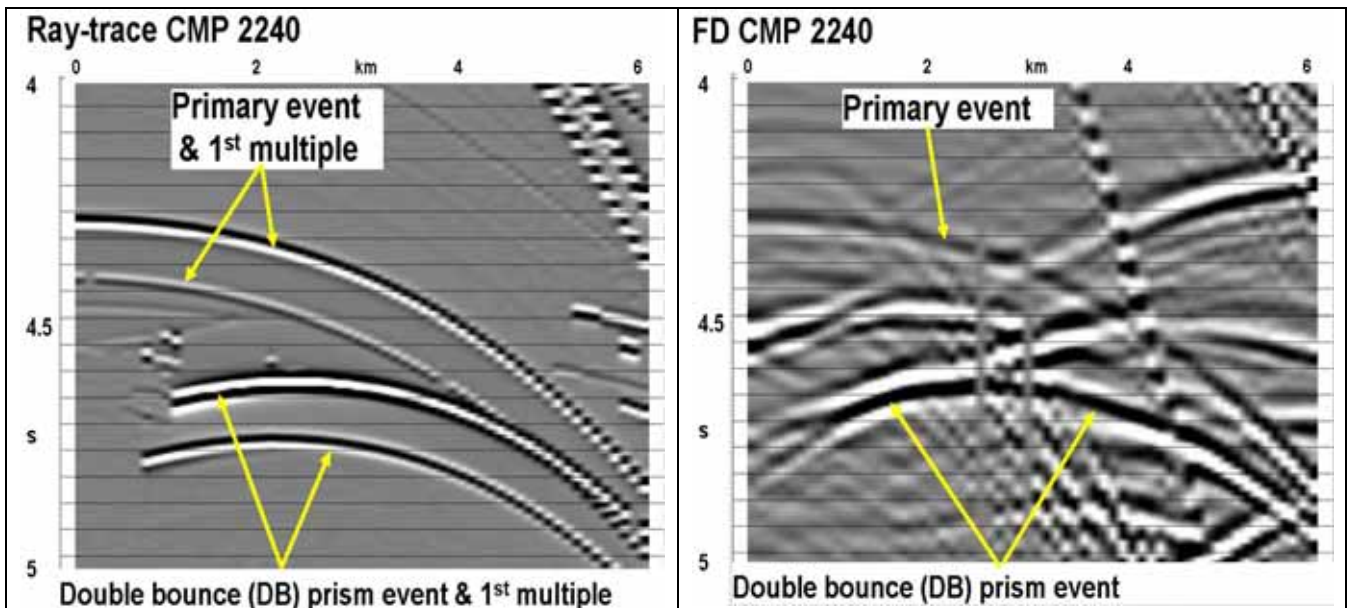


Figure 7b. Detail of CMP stacked sections for the ray-traced synthetic data as well as the FD data (from box indicated in figure 7) showing location of double bounce events in diffraction tails. Also noted is the location of CMP 2240. For this study we have not performed any stacking velocity analysis, hence the data have been stacked simply using the RMS version of the interval velocity model.



Figures 8 & 9 a CMP (model location 2240), for the acoustic ray-traced data with double bounces (also including the free-surface multiple), and the elastic FD data (without free surface multiples).

Pre-Processing

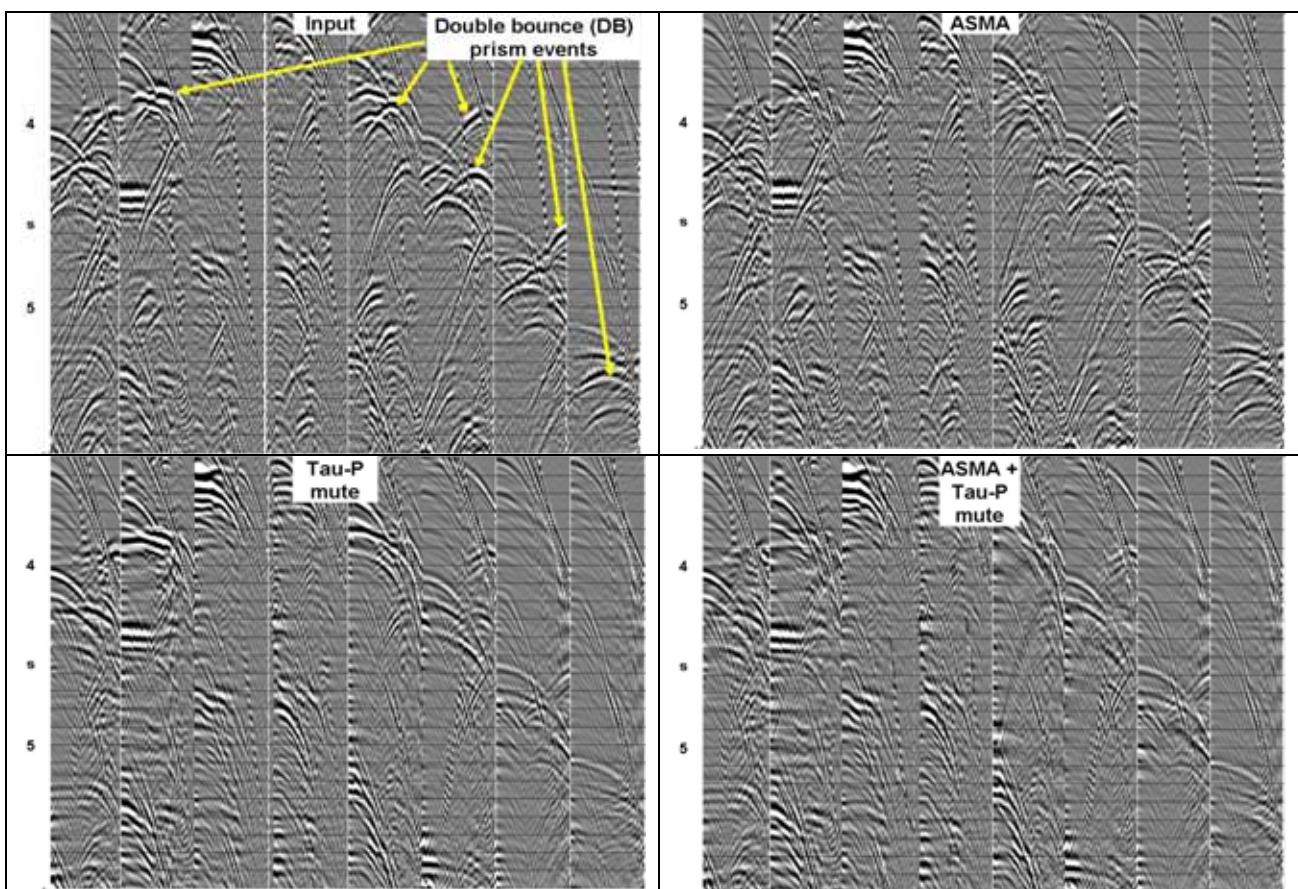
Essentially, we are looking at processes that eliminate events which exhibit ‘anomalous’ moveout behaviour in the CMP domain. For conventional 2D geometry, such events (in a one-way wave propagation paradigm) constitute diffracted multiples and scattered energy. In other words, events that appear to have secondary source locations from a one-way perspective. Such events are classes of two-way wave propagation, in that the ray-path changes direction before (or after) its ‘main’ reflection from the interface of interest.

We commenced by assessing Radon demultiple. If we were to employ the Radon filter to directly output the multiple free ‘primaries’, then we would have a problem, as all apex-shifted events would be corrupted, appearing as a smeared artefact in the output. However, this issue can be circumvented if we use the Radon to model the multiples, and then adaptively subtract these from the input data. Working in this way, we would preserve the apex-shifted arrivals in the CMP gather. Consequently, we do not show the Radon results here.

We then assessed an apex shifted multiple attenuation routine ‘ASMA’ - designed to attenuate events whose apexes are shifted from zero offset in CMP gathers: as a first order approximation to 3D SRME. By design, this effectively eradicates the double bounce events.

Lastly, we assessed a Tau-P mute (for backscattered noise). Normally, this is performed in conjunction with a deconvolution. Here we have not applied the deconvolution step, so as to isolate and highlight the effect of the Tau-P mute (also, as we used an absorbing surface boundary condition in the FD modelling, we don’t have direct short-period water bottom multiples in the E3D data)

We show the effects of these processing sequences in the following figures, for a set of CMP gathers straddling the salt dome. Figure 10 shows the raw input FD modelled data, whilst figures 11 - 13 show the outputs from ASMA, Tau-P muting, and both these processes. Apex shifted events are ‘successfully’ attenuated. This would be considered a good thing for conventional processing, but is deleterious for two-way imaging.



Figures 10 - 13: selection of gathers with 6km maximum offset from the FD modelled data, showing the raw input, and the outputs from ASMA (fig. 11) which has performed slightly better than Tau-P on the left of the section, Tau-P muting which has performed better on the right (fig. 12), and both these processes. Apex shifted events are ‘successfully’ attenuated. This would be considered a good thing for conventional processing.

Effects on RTM migration

In figure 14 we see the RTM of the FD raw data using a slightly smoothed model, and post-processing to enhance the image. However, in an industrial flow, where we are trying to determine the model, we would approach the definition of the salt flank using a migration with a salt-free model. In RTM, the imaging condition will still produce an image of the salt flank from double bounce events as long as the flat-lying high velocity contrast layers are present in the model. So, in order to evaluate the effect of our pre-processing on the imaging of the double bounce arrivals, we compare results using RTM with a no-salt model. Figure 15 shows the image of the raw data with the no-salt model. In both figures 14 & 15 the interval velocity model used in the migration is superimposed. Figure 16 repeats the previous figure, but without the colour model overlay, and figure 17 shows the RTM image using the no-salt model of the data subjected to Tau-P mute and ASMA. It is clear that the vertical and overturned salt-flank events have been seriously attenuated in the latter sequence.

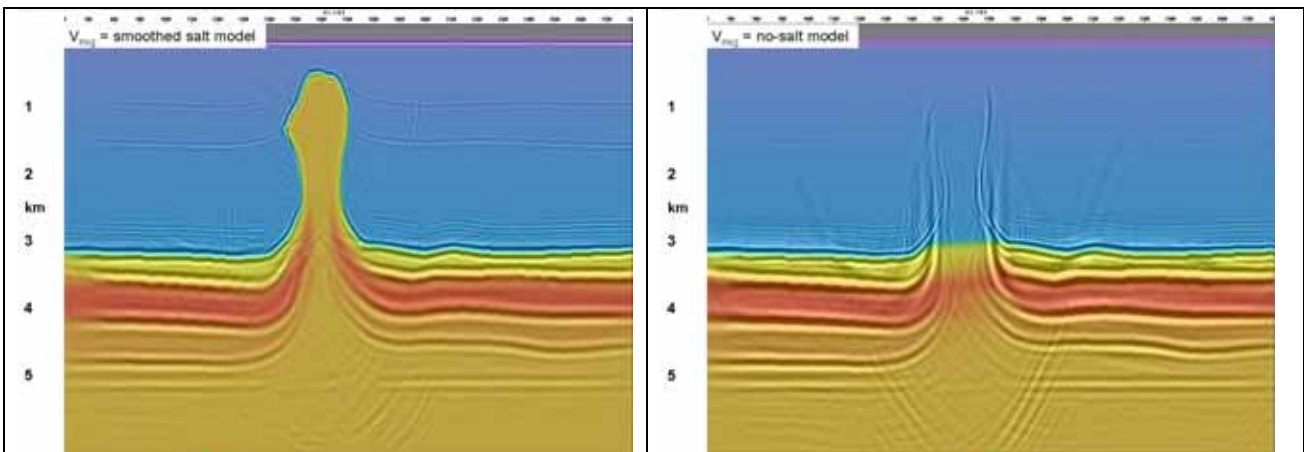
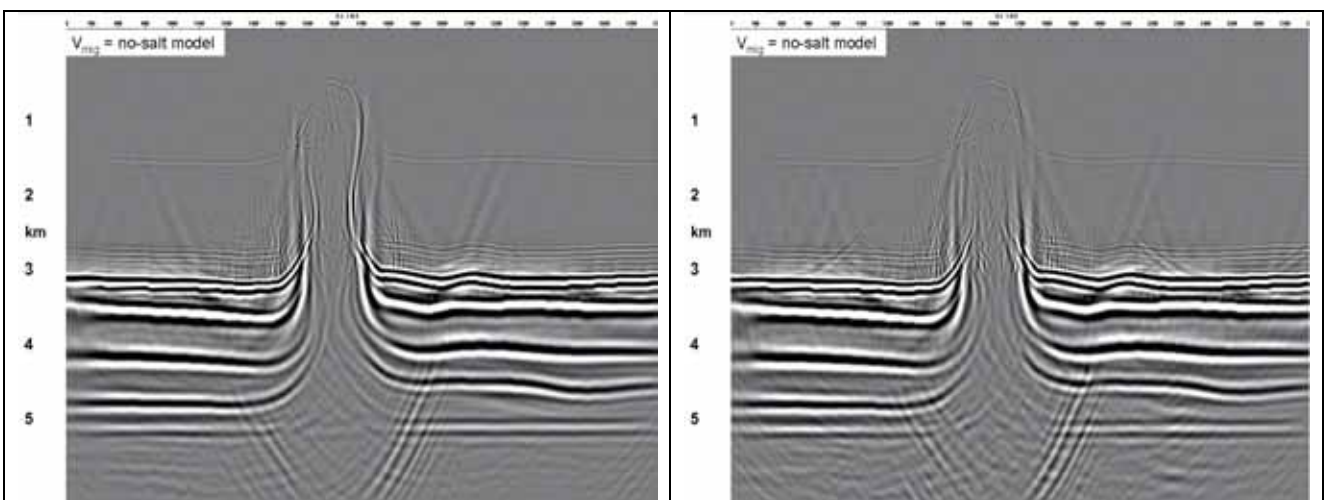


Figure 14: RTM with raw data and salt model. Figure 15: RTM with raw data and no-salt model. The salt wall image looks nicer in the no-salt model as we avoid the (correct) model imposed wavelet stretch at the salt boundary. The imaging condition still constructs the salt-wall event, as we have one bounce-point specified in the model (the flat lying top Balder).



Figures 16 & 17. RTM images of the raw data (as per the previous figure, but without the superimposed model) and the data processed with ASMA and Tau-P muting. The overturned salt wall reflectors have been significantly damaged by this conventional pre-processing flow.

Real Data

Having demonstrated the deleterious effects of inappropriate pre-processing on RTM imaging using the synthetic data, we now consider a real North Sea example. In fact it was the mixed success of RTM migration on such salt structures that alerted us to the issues described here. On one project

(Farmer, et al, 2006) the results were impressive, however, on a subsequent project involving a neighbouring salt dome with similar geology and similar acquisition, the results of RTM were disappointing (in-part perhaps due to model inaccuracies, but possibly also due to the effects of slightly different pre-processing).

Here we have revisited the successful project (for which we have show-rights) and re-worked the pre-processing to attempt to assess the damage done by typical production pre-processing. In the production project mentioned, conducted in 2005 - 2006, serendipitously no deleterious pre-processing was applied. In the unsuccessful project, a Tau-P mute was used to attenuate problematic back-scattered noise. Here we have taken this same Tau-P mute and applied it to data from the first (successful) project. The tests have been conducted only in 2D, using a crestal line, but the conclusions are valid for the 3D case.

In figure 18, we see the input data along the selected crestal line, and in figure 19, the anisotropic 3D RTM of these data with an intermediate (no-salt) model, highlighting the double bounce events (Farmer, et al 2006).

In figure 20, we see the input CMP gathers, with maximum offset 3100m, as used in the successful production project (and to make the stack shown in figure 18). In figure 21, we have applied a Tau-P mute designed to remove 'backscattered' energy: in this case we note that it damages events with shifted apices. From the perspective of conventional processing, this result would normally be considered good, but as we now know, it will prove damaging to RTM.

In figure 22, we show the 2D RTM of SRME data using a no salt model We see double bounce energy arrivals appearing as near-vertical events in the vicinity of the salt flanks. Figure 23, shows the RTM image with the same model, but using as input the data after the Tau-P mute. The double bounce energy has been removed. In both figures, there is an inset of a CMP gather showing the data going in the migration. It is evident that double bounce events are removed by the Tau-P mute, as they resemble back-scattered energy, appearing with a shifted apex in the CMP domain.

Conclusions

Conventional pre-processing is designed to remove various classes of noise, such as backscattered energy, multiples, and diffracted multiples. The processes designed to do this, have for the most-part, been designed with one-way wave propagation of primary energy in-mind.

Software developers have spent several years developing these routines that will efficiently remove diffracted multiples and back-scattered noise, developing the apex-shifted approach and more recently 3D SRME.

However, if we set-out to migrate two-way propagated primary energy, as is now possible with the new generation of migration algorithms (such as RTM), we need to ensure that our pre-processing flow is 'fit-for-purpose', and does not inadvertently damage the very events we are trying to image.

Typically, two-way propagated primary events (such as double bounces), appear in the CMP domain with their moveout apex shifted from zero offset. As such, they resemble diffracted multiples or backscattered energy.

Consequently, tools such as 3D SRME must be employed instead of more conventional 2D approaches when dealing with multiple suppression in complex environments, so as to avoid unnecessary removal of useful primary (two-way) energy.

Acknowledgements

I wish to thank my colleagues at ION GX Technology for useful discussions, and especially Mike Goodwin, Stuart Greenwood, and Brent Mecham, for help creating the synthetic data, and to Dave King, Mick Sugrue, and Ivan Berranger for discussions and help with the RTM jobs. Thanks also to the management of ION GX Technology, for permission to publish the results of this study.

References

- Baysal, E., Kosloff, D. D. and Sherwood, J. W. C., 1983, Reverse time migration: *Geophysics, Soc. of Expl. Geophys.*, 48, 1514-1524.
- Bednar, J.B., Yoon, K., Shin, C. and Lines, L. R., 2003, One Way vs Two Way Wave Equation Imaging – Is Two-Way Worth It?, 65th Mtg.: *Eur. Assn. Geosci. Eng.*, B11
- Bernitsas, N., Sun, J., and Sicking, C., 1997: Prism waves – an explanation for curved seismic horizons below the edge of salt bodies, 59th Ann. Internat. Mtg. *Europ. Assoc. Expl. Geophys.*
- Cavalca, M., and Lailly, P., 2005, Prismatic reflections for the delineation of salt bodies, 75th Ann. Internat. Mtg: *Soc. of Expl. Geophys.*
- Davison, I., Alsop, G.I., Evans, N.G., Safaricz, M., 2000, Overburden deformation patterns and mechanisms of salt diapir penetration in the Central Graben, North Sea. *Marine and Petroleum Geology*, 17, p601-618.
- Farmer, P., Jones, I.F., Zhou, H., Bloor, R., and Goodwin, M.C., 2006, Application of Reverse Time Migration to Complex Imaging Problems. *First Break*, v24, No.9, p65-73.
- Hale, D., N. R. Hill, and J. Stefani, 1992, Imaging salt with turning seismic waves : *Geophysics*, **57**, no.11, 1453-1462
- Hawkins, K., Cheng, C.-C., Sadek, S. A., and Brzostowski, M. A., 1995, A $v(z)$ DMO developed with the North Sea Central Graben in mind: 65th Annual International Meeting, SEG, Expanded Abstracts , 1429-1432.
- Jones, I.F., 2008, A Modeling Study of Pre-Processing Considerations for Reverse Time Migration, *Geophysics*, in prep.
- Larsen, S. C., and J. C. Grieger, 1998, Elastic modeling initiative, Part III: 3-D computational modeling: 68th Annual International Meeting, SEG, Expanded Abstracts, 1803-1806
- Levander, A. R., 1988, Fourth-order finite-difference P-SV seismograms: *Geophysics*, **53** , no.11, 1425-1436.
- Madariaga R., 1976, Dynamics of an expanding circular fault: *Bulletin of the Seismological Society of America*, 66: 639-666
- McMechan, G.A., 1983, Migration by extrapolation of time-dependent boundary values: *Geophysical Prospecting*, 31,413-420.
- Mittet, R., 2006, The behaviour of multiples in reverse time migration, 68th Ann. Internat. Mtg. *Eur. Assn. Geosci. Eng.*,
- Shan, G., and Biondi, B., 2004, Imaging overturned waves by plane wave migration in tilted coordinates: 74th Annual International Meeting, SEG, Expanded Abstracts, 969-972.
- Thomson, K., 2004, Overburden deformation associated with halokinesis in the Southern North Sea: implications for the origin of the Silverpit Crater. *Vis Geosci*, 9, p1-9.
- Virieux, J., 1986, P-SV wave propagation in heterogeneous media - Velocity-stress finite-difference method: *Geophysics*, **51** , no.4, 889-901
- Whitmore, N. D., 1983, Iterative depth migration by backward time propagation: 53rd Annual International Meeting, SEG, Expanded Abstracts, Session: S10.1.
- Yoon, K., Shin, C., Suh, S., Lines, L. R. and Hong, S., 2003, 3D reverse-time migration using the acoustic wave equation: An experience with the SEG/EAGE data set: *The Leading Edge*, 22, no. 1, 38-41
- Zhou, H., Zhang, G., and Bloor, R., 2006, Anisotropic Acoustic Wave Equation for VTI Media, 68th Ann. Internat. Mtg. *Eur. Assn. Geosci. Eng.*,
- Zhang, Y., Sheng, X., and Zhang, G., 2006, Imaging complex salt bodies with turning-wave one-way wave equation. SEG/EAGE summer research workshop, Utah.

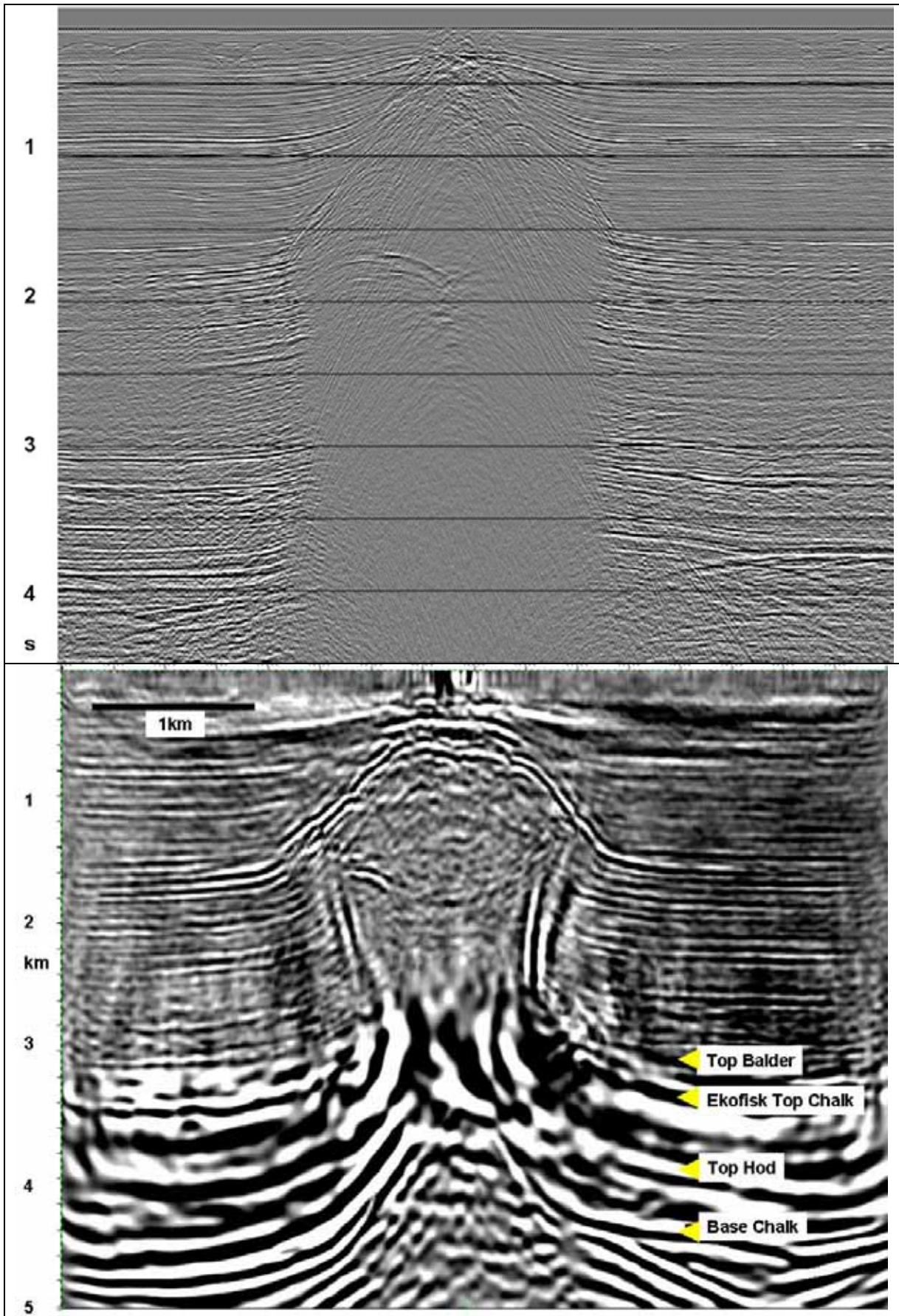


Figure 18. Stack of CMP's as input to the successful project. Figure 19, intermediate anisotropic 3D RTM result with a no-salt model.

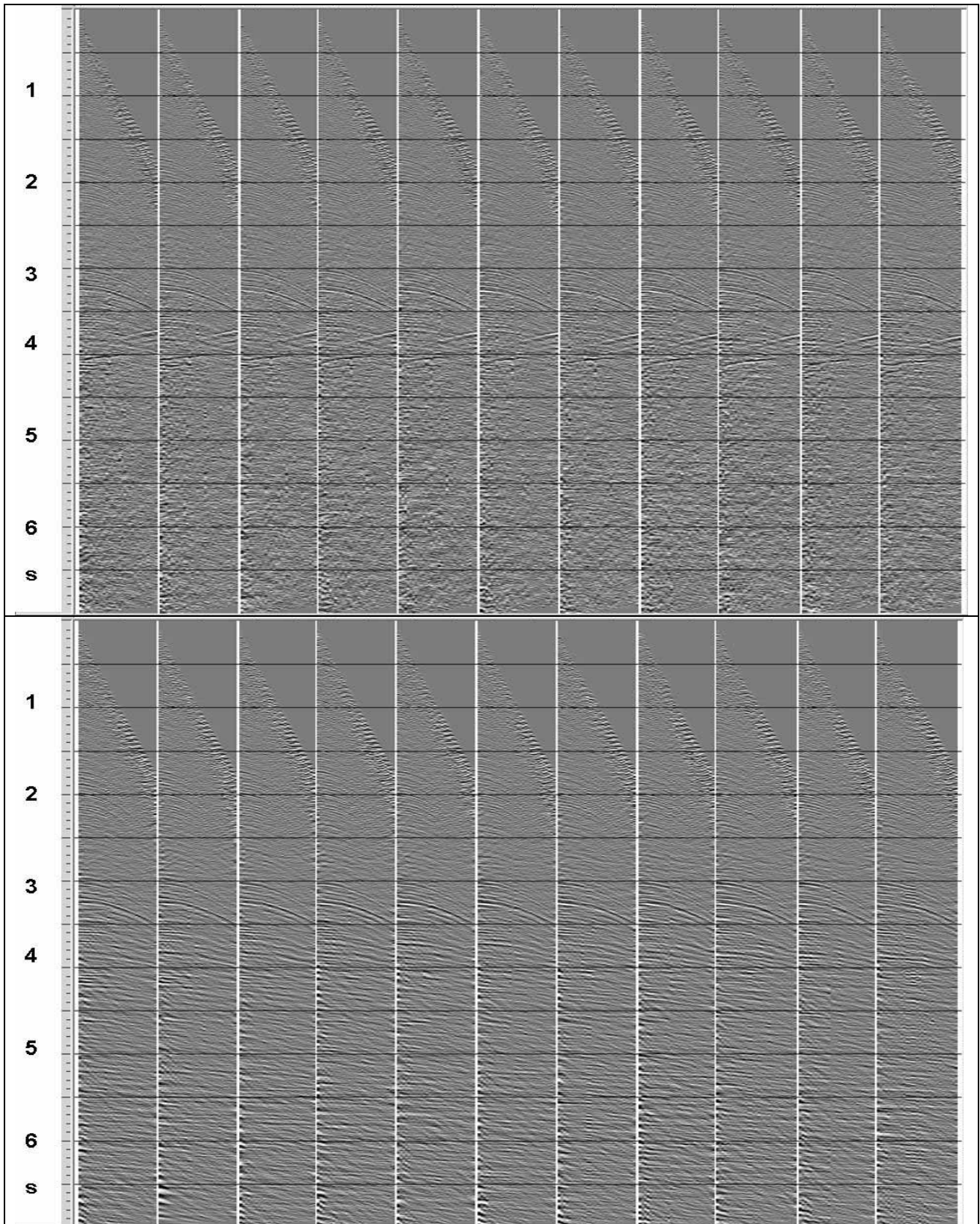


Figure 20. CMP gathers (with maximum offset 3100m) input to the successful project. Figure 21, CMP gathers after application of a Tau-P domain mute designed to attenuate back-scattered energy (thus affecting shifted apex CMP events). The contra-dipping events have been suppressed. These are suspected to be double bounce arrivals.

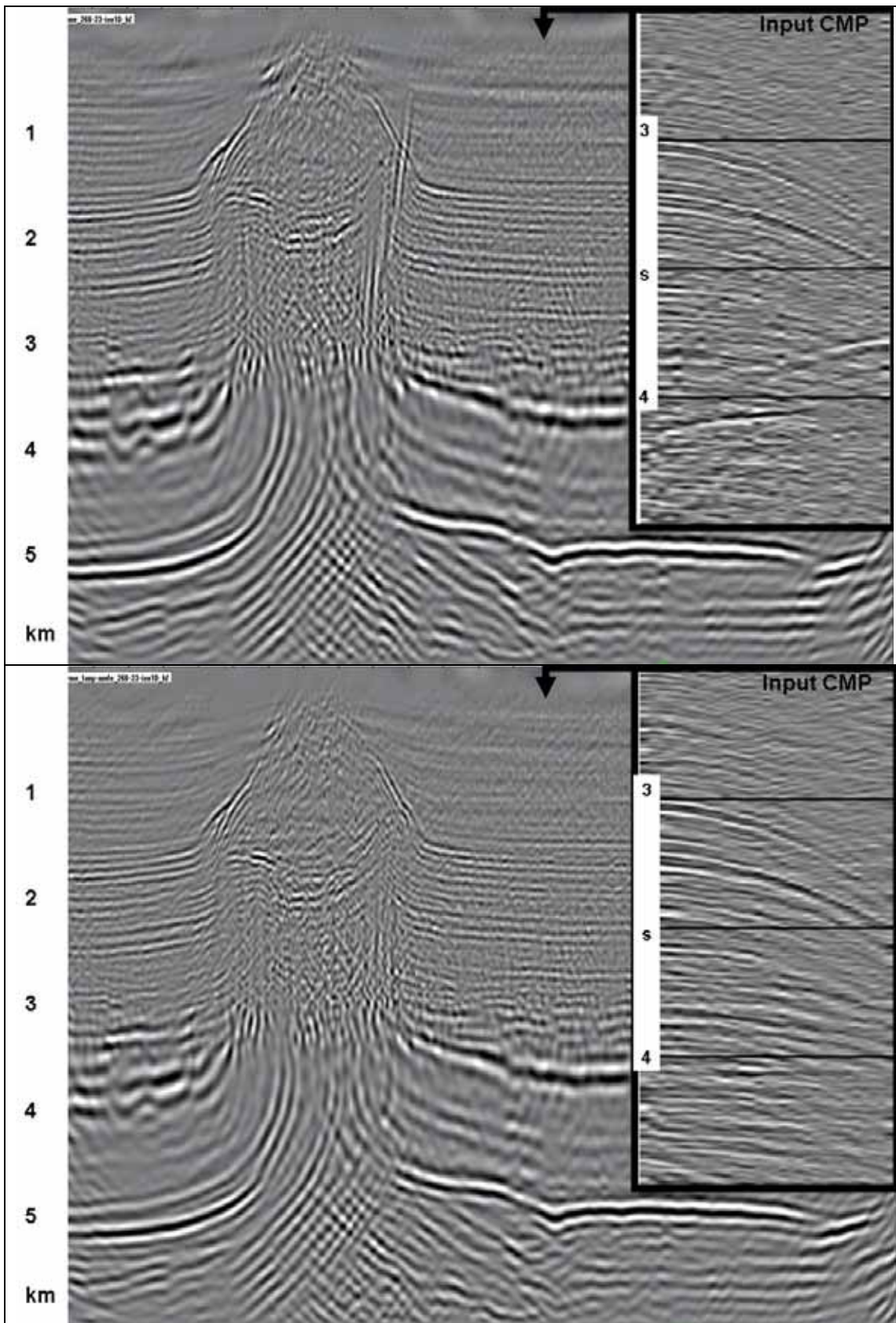


Figure 22. Isotropic 2D RTM of SRME data using a no salt model. We see double bounce energy arrivals appearing as near-vertical events in the vicinity of the salt flanks. Figure 23, RTM with the same model, but using as input the data after the Tau-P mute. The double bounce energy has been removed. In both figures, there is an inset of a CMP gather showing the double bounce events which are removed by the Tau-P mute, as they resemble back-scattered energy, appearing with a shifted apex in the CMP domain.